Variation of Jupiter's Aurora Observed by Hisaki/EXCEED: 4. Quasi-Periodic Variation

Chihiro Tao[1], Tomoki Kimura[2], Elena A. Kronberg[3], Fuminori Tsuchiya[2], Go Murakami[4], Atsushi Yamazaki[5], Marissa F. Vogt[6], Bertrand Bonfond[7], Kazuo Yoshioka[8], Ichiro Yoshikawa[9], Yasumasa Kasaba[2], Hajime Kita[10], and Shogo Okamoto[11]

[1]National Institute of Information and Communications Technology (NICT)
[2]Tohoku University
[3]Ludwig Maximilian University of Munich
[4]Japan Aerospace Exploration Agency
[5]Institute of Space and Astronautical Science
[6]Boston University
[7]Université de Liège
[8]The University of Tokyo
[9]University of Tokyo
[10]Tohoku Institute of Technology
[11]Nagoya University

November 23, 2022

Abstract

Quasi-periodic variations of a few to several days are observed in the energetic plasma and magnetic dipolarization in Jupiter's magnetosphere. Variation in the plasma mass flux related to Io's volcanic activity is proposed as a candidate of the variety of the period. Using a long-term monitoring of Jupiter by the Earth-orbiting space telescope Hisaki, we analyzed the quasi-periodic variation seen in the auroral power integrated over the northern pole for 2014–2016, which included monitoring Io's volcanically active period in 2015 and the solar wind near Jupiter during Juno's approach in 2016. Quasi-periodic variation with periods of 0.8–8 days was detected. The difference between the periodicities during volcanically active and quiet periods is not significant. Our dataset suggests that a difference of period between this volcanically active and quiet conditions is below 1.25 days. This is consistent with the expected difference estimated from a proposed relationship based on a theoretical model applied to the plasma variation of this volcanic event. The periodicity does not show a clear correlation with the auroral power, central meridional longitude, or Io phase angle. The periodic variation is continuously observed in addition to the auroral modulation due to solar wind variation. Furthermore, Hisaki auroral data sometimes shows particularly intense auroral bursts of emissions lasting <10h. We find that these bursts coincide with peaks of the periodic variations. Moreover, the occurrence of these bursts increases during the volcanically active period. This auroral observation links parts of previous observations to give a global view of Jupiter's magnetospheric dynamics.

Title: Variation of Jupiter's Aurora Observed by Hisaki/EXCEED: 4. Quasi-Periodic Variation
Paper: JGR, Space Physics

Authors: Chihiro Tao [1], Tomoki Kimura [2], Elena A. Kronberg [3], Fuminori Tsuchiya [2], Go Murakami [4], Atsushi Yamazaki [4], Marissa F. Vogt [5], Bertrand Bonfond [6], Kazuo Yosihoka [7], Ichiro Yoshikawa [7], Yasumasa Kasaba [2], Hajime Kita [8], and Shogo Okamoto [9]

Affiliations:
[1] National Institute of Information and Communications Technology (NICT), Tokyo, Japan
[2] Tohoku University, Japan
[3] Department of Earth and Environmental Sciences, University of Munich, Germany
[4] ISAS/JAXA, Japan
[5] Boston University, USA
[6] Universite de Liege, Belgium,
[7] The University of Tokyo, Japan
[8] Tohoku Institute of Technology, Japan
[9] Nagoya University, Japan

Corresponding Author: Chihiro Tao (chihiro.tao@nict.go.jp)
Running title (<=45 characters): Jupiter's intrinsic variation seen via aurora
Abstract&text ~6300 + Figure caption 700 = ~7000 -> unit 14
Figure 10 + Table 0
UNIT= 14+10=24 <= 25

Key points (<=140 characters):
1. Quasi-periodic variations of a few to several days seen in Jupiter's polar-integrated northern aurora observed by Hisaki
2. Auroral bursts <10 h sometimes seen at peak of periodic variation, whose occurrence increases with Io's volcanic activity
3. This periodic variation additionally seen in aurora intensity enhancements associated with solar wind variations
----

Abstract

[1] Quasi-periodic variations of a few to several days are observed in the energetic plasma and magnetic dipolarization in Jupiter's magnetosphere. Variation in the plasma mass flux related to Io's volcanic activity is proposed as a candidate of the variety of the period. Using a long-term monitoring of Jupiter's northern aurora by the Earth-orbiting planetary space telescope Hisaki, we analyzed the quasi-periodic variation seen in the auroral power integrated over the northern pole for 2014–2016, which included monitoring Io's volcanically active period in 2015 and the solar wind near Jupiter

during Juno's approach phase in 2016. Quasi-periodic variation with periods of 0.8–8 days was detected. The difference between the periodicities during volcanically active and quiet periods is not significant. Our dataset suggests that a difference of period between this volcanically active and quiet conditions is below 1.25 days. This is consistent with the expected difference estimated from a proposed relationship based on a theoretical model applied to the plasma variation of this volcanic event. The periodicity does not show a clear correlation with the auroral power, central meridional longitude, or Io phase angle. The periodic variation is continuously observed in addition to the auroral modulation due to solar wind variation. Furthermore, Hisaki auroral data sometimes shows particularly intense auroral bursts of emissions lasting <10 h. We find that these bursts coincide with peaks of the periodic variations. Moreover, the occurrence of these bursts increases during the volcanically active period. This auroral observation links parts of previous observations to give a global view of Jupiter's magnetospheric dynamics.

1. Introduction

[2] Jupiter's huge magnetosphere shows quasi-periodic variations with periods of a few to several-day. Long-term observation by the Galileo spacecraft shows the periodic variation of the energetic ion flux and spectral slope in the vast magnetospheric region beyond 20 R_J (R_J is Jupiter's radius) and various local time [e.g., Woch et al., 1998; Kronberg et al., 2009]. Periodic reconfiguration of the magnetosphere between a loading phase involving thinning of the magnetospheric current sheet for ~2 days and an unloading phase associated with dipolarization of the magnetic field for ~1 days was proposed by Woch et al. [1998]. Statistical analysis of the magnetic field observed by Galileo showed a reconnection-like variation with 1–4 days intervals for some orbits [Vogt et al., 2010]. Polar-integrated aurora observed by International Ultraviolet Explore (IUE) showed variations by a factor of 2–4 in time scales of 5–10 days [Prangé et al., 2001]. They found that this periodic variation corresponds to the variation of the magnetic field between quiet and disturbed days observed in Jupiter's magnetotail by the Galileo magnetometer (MAG). Louarn et al. [2014] reported the

enhancement of auroral radio flux (hectometric emission, HOM) and the initiation of a radio source in the Io plasma torus (IPT) (narrow-band kilometric emission, nKOM) almost simultaneously with the periodic events of energetic ions and plasma injection features. The appearance and disappearance of the auroral spot observed by Hubble Space Telescope (HST) in the poleward region of the dawnside main emission also show variation with a period of 2–3 days [Radioti et al., 2010]. A similar spot has been suggested to be a precursor of the auroral intensification [Gray et al., 2016].

[3] There are various periodicities with a similar time scale, but it is unknown what controls the variation. Io's volcanic activity is one of the candidates via changing the plasma mass flux in the magnetosphere. Io provides a massive plasma outflow consisting of sulfur and oxygen ions as main contributors to the plasma pressure, which balances with the magnetic pressure in Jupiter's magnetosphere. Kronberg et al. [2007] proposed a theoretical model to quantitatively explain the variation of periodicity that was based on magnetic field and plasma observations. They found theoretically that the time constant of the Jovian magnetosphere needed for mass loading until reconnection onset decreases with increasing plasma mass flux, although this has not been confirmed by observations. The contribution of solar wind variation is also under debate. Kronberg et al. [2008] and Yao et al. [2019] suggested that the periodic variation seen in the energetic plasma flux and magnetic field is independent of the solar wind variation. Vogt et al. [2019] analyzed plasma and magnetic field observations by Galileo in Jupiter's magnetotail and suggested two types of variations, (i) magnetospheric compression events due to variation of solar wind dynamic pressure and (ii) tail reconnection and plasmoid release, most likely internally driven by the Vasyliunas cycle [Vasyliunas, 1983].

[4] The Hisaki Earth-orbiting space telescope monitors both the IPT and Jupiter's northern aurora simultaneously [Yoshioka et al., 2013; Yoshikawa et al., 2014; Yamazaki et al., 2014; Kimura et al., 2019]. Although the EXCEED (Extreme Ultraviolet Spectroscope for Exospheric Dynamics) spectrometer cannot resolve the auroral structure due to its moderate spatial resolution (about 1 R_J at

Jupiter's opposition), it provides auroral spectra continuously for ~40 min during each 106-min orbit. Since its launch in 2013, Hisaki has observed Jupiter for several months around its oppositions. In this study, we analyze the periodic variation of the aurora observed by EXCEED using 2014–2016 data, which includes monitoring a volcanically active event in 2015 [e.g., Yoshikawa et al., 2017; Tsuchiya et al., 2018; Tao et al., 2018; Kimura et al., 2018] and solar wind during Juno's approaching phase.

2. Observations and Data Procedure

[5] The Hisaki observations and auroral analysis are outlined briefly here; for details of the observations and data reduction, see Kimura et al. [2019], and for the analysis of the auroral spectra, see Tao et al. [2016a; 2016b]. The northern auroral region is covered by the central thin part of a dawn-dusk directed dumbbell-shaped 140 arcsec slit with an effective spatial resolution of 17 arcsec. EXCEED detects part of the H_2 Lyman and Werner band emissions over the 80–148 nm wavelength range with full width at half maximum (FWHM) resolution of 0.4 nm. The auroral signals within the 20 arcsec aperture of the slit width are integrated over specific wavelength ranges. The waveband 138.5–144.8 nm is used to estimate the total auroral emission and input power. The far-ultraviolet color ratio (CR) is defined as the ratio of the intensity of the waveband absorbed least by atmospheric hydrocarbons (138.5–144.8 nm) to that absorbed most (123–130 nm), which for EXCEED is defined as CR_{EXCEED}. As the CR reflects the depth of the auroral electron precipitation into the hydrocarbon layer, the auroral electron energy can be estimated assuming the atmosphere model. The total number flux is derived from the electron energy and energy flux. The source current density can be estimated with reference to the auroral electron acceleration theory [Tao et al., 2016b]. We analyze the observation when the Jupiter northern aurora was facing to Earth, i.e., when the central meridional longitude (CML) was 45–345° system III longitude. Since the northern auroral oval is non-axisymmetric surrounding the magnetic pole, which is shifted from Jupiter's rotational pole, the auroral power detectable from Earth varies with Jupiter's rotation. This power variation due to the appearance is scaled by multiplying by the factor (auroral area integrated over all longitude)/(visible

auroral area at instantaneous CML), assuming a typical auroral location. The appearance-corrected power is obtained as shown in Figure 1a. Auroral observation is integrated over 10 minutes to increase the signal to noise ratio.

[6] Quasi-periodic variation of the aurora is detected automatically as follows. First, we obtain a temporal sequence of the median of the power in the waveband 138.5–144.8 nm within a 0.5-day window shifted by 0.25 day (green line in Figures 1a and 1b). Then we take a 3-point running average, i.e., over 0.75 day (thick grey line in Figure 1b) and obtain its time deviation, d(Power)/dt (black line in Figure 1c). We select events with positive d(Power)/dt with a duration of 0.5 day or more (orange points in Figures 1b and 1c) and negative d(Power)/dt with a duration of 0.5 day or more (blue points in Figures 1b and 1c). In order to exclude small perturbations, such as those around day of year (DOY) 25 in 2015 (Figure 1), whose amplitudes are insufficient to discuss the periodicity, only cases satisfying $\Sigma(|d(Power)/dt|)>28$ GW/day summed over the positive and negative deviations are picked up. The detected events are shown by vertical purple lines at the peak of each event in Figures 1a and 1b. After excluding events with lacking data of ≥0.5 day in the interval, we obtain the temporal interval between the brightness peaks of the quasi-periodic events ("*dt*" hereinafter).

[7] We also investigate the amplitude of the periodic variation and the existence of bursty auroral brightening with short durations of <10 h. The amplitude of each variation is estimated from the difference between the maximum and minimum of the running averaged power, as shown by thick black lines in Figure 2b. If the maximum value during each periodic brightness peak (diamonds in Figure 2b) is above the maximum of the running average (green line) by 1.5σ or more, where σ is the error estimated from the photon statistics, we label it as a periodic event with a significant auroral burst. For example, enhancements on DOY ~4, 11, 15, and 17 in 2014 are detected as significant auroral bursts as shown by red vertical lines in Figure 2b, while the others on DOY 1, 5, 21, and 23 are periodic variations without significant bursts as shown by blue vertical lines.

[8] We compare the periodic variation with the external solar wind observed by Juno during its approaching phase toward Jupiter. Solar wind dynamic pressure is considered to be an important parameter that affects Jupiter's magnetosphere, as investigated in many studies [e.g., Vogt et al., 2019; Nichols et al., 2017, Kita et al., 2019]. During Juno's solar wind plasma observation from May to July 2016, the continuity of Hisaki observation was not adequate for automatic analysis. Compressed magnetic field structures of the interplanetary magnetic field (IMF) are often associated with enhancements of solar wind dynamic pressure. We refer to the IMF observation by the magnetometer (MAG) [Connerney et al., 2017] on board Juno for the solar wind information to cover January and February 2016. We use MAG data with a time resolution of 60 s taken from the NASA Planetary Data System (PDS) website. The IMF variation observed at the Juno spacecraft is shifted to the location of Jupiter assuming a solar wind velocity of 400 km/s [e.g., Wilson et al., 2018] and a constant structure during the solar rotation. This simple estimation is applicable since Juno was close to Jupiter, within 0.12 AU and 6.2° separation in heliospheric radius and longitude, respectively, for DOY 20–63 in 2016.

3. Results

[9] Figure 3 shows an overview of the dataset analyzed in this study. Hisaki is continuing its observation of Jupiter's aurora (even now in August 2020), while we use highly continuous data until the middle (DOY 241) of 2016 to detect the periodic variation automatically. Top plots show the auroral power in the 138.5–144.8 nm band, which reflects the total input power. Detected periodic variations are indicated by red or blue lines at their peaks in the top plots and their separation interval *dt* is shown in middle plots. This dataset covers quiet (from DOY 1 in 2014 to DOY20 in 2015) and large active volcanic event (DOY 20–100 in 2015) as seen in the variation of S^+ emission from the IPT (bottom plots). Since some sporadic volcanic activities occurred in 2016, i.e., DOY ~140 [Kimura et al., 2017; Tsuchiya et al., 2019], we exclude the 2016 dataset from the comparison of behaviors between volcanically quiet and active time.

[10] Figure 4 shows a histogram of the separation interval of the auroral periodic variation *dt*. The interval over the whole analyzed period varies in the range of 0.8–11.5 days with a peak at 2 days. The analyses applied to Io's volcanically quiet (from DOY 1 in 2014 to DOY 40 in 2015) and active (DOY 40–140 in 2015) periods are shown by dotted and dot-dashed lines, respectively, which are concentrated at a similar separation time. The mean and standard deviation during the quiet (active) period are 3.0 (2.6) and 1.3 (1.0) days, respectively. For the quiet period, we excluded the extreme event at dt=11.5 days. We use the Mann–Whitney U-test to investigate whether two independent samples taken from non-normal populations have the same distribution. Excluding the extreme event, the null hypothesis, i.e., (dt during the active period) = (dt during the quiet period), is not rejected by the Mann–Whitney U-test (test statistics: U=249.5, z=1.05, p=0.290, sample size n=40). See Section 4.3 for the power analysis.

[11] An interesting finding from this analysis is that the auroral bursts sometimes occurred at the peaks of the periodic variation, several examples of which are shown in Figure 2. The events on DOY ~4, 11, and 15 in 2014 are auroral bursts reported by Kimura et al. [2015]. The first two events were almost simultaneously observed with HST. The auroral images taken by HST show low-latitude expansion and blobs along the main aurora [Kimura et al., 2015; Badman et al., 2016]. These events were seen at the peak of the periodic variation. There are also periodic variations that are not associated with significant auroral bursts: e.g., DOY 1, 5, 21, and 23 in 2014 in Figure 2.

[12] The existence (red) and absence (blue) of the auroral bursts over the whole period shows concentrations of the occurrence of these events, e.g., DOY ~10 and ~355 in 2014, 40–120 in 2015, and 20–50 in 2016. On the other hand, the quasi-periodic variation is seen almost all the time. The longest period in which the periodic variation coincided with the auroral burst, DOY 40–120 in 2015, corresponds to Io's volcanically active event. The number of events associated with significant power enhancements is 16 (17) within 39 (26) periodic variations, i.e., an occurrence ratio of 41% (65%), for the volcanically quiet (active) period from DOY 1 in 2014 to DOY 40 in 2015 (DOY 40–140 in 2015).

[13] Figure 5 shows the relationship between the separation interval and geometric parameters and auroral powers. There is not clear correlation between *dt*, CML (Figure 5a), Io phase angle (Figure 5b), and the amplitude of the periodic variation (Figure 5c) which would reflect the size of magnetospheric reconfiguration (see Section 4.2). The same analysis using different Io volcanic activity levels also shows no clear correlation if the extreme event $dt > 8$ is excluded. On the other hand, we found a significant positive correlation between the amplitude power and auroral burst power. The amplitude power corresponds to the maximum difference of power within a periodic variation (e.g., the size of thick black lines in Figure 2b), while the auroral burst power is the excess of auroral burst (e.g., diamonds in Figure 2b) from the peak power of the periodic variation. The correlation coefficient is 0.49 for the dataset using the whole period, and 0.64 and 0.69 for Io volcanically active and quiet times, respectively.

[14] Superposed-epoch analysis is carried out for the observed power and the estimated parameters from the spectral analysis. The timing of the power peaks of the quasi-periodic variation is set to time=0 as enhancement is seen in the auroral power (Figure 6a). The mean value of all events within each time bin is shown in red. If we exclude the periodic events associated with the auroral bursts, the mean value (blue) at time=0 decreases, while this purely reflects the periodic variation. CR_{EXCEED} shows a slight decrease from ~1.4 to ~1.3; this decrease is smaller than their variance ~0.4 (Figure 6b). This decrease around time=0 is less clearly seen if the auroral burst events are excluded (blue, Figure 6b). In contrast to the variation in CR_{EXCEED}, the source current is enhanced from ~3 to ~7 nA/m^2 with increasing auroral power (Figure 6c). Since the absolute values of these parameters vary among events, we conducted similar analysis using the variation ratio of each parameter normalized by the initial value of each periodic variation, as shown in Figures 6d–6f. Increasing and decreasing trends are more clearly seen in the power and current density. This periodic variation of auroral power is mainly related with the change in source current. The source current varies with the periodic variation by a factor of ~1.6 (Figure 6f).

[15] We statistically investigate the durations of increasing and decreasing power over in the quasi-periodic variation. The duration of increasing (decreasing) vary from 0.5 to 2.25 days (0.25 to 2.75 days) with mean and standard deviation values of 0.96±0.39 (0.78±0.52) days for the whole period as shown in Figure 7a (Figure 7b). The difference between the durations of increasing and decreasing auroral power is significant according to the Mann–Whitney U-test ($U=4401.5$, $z=4.03$, $p=5.4\times10^{-5}$, $n=225$). The histogram of the duration differences shows a slightly longer increasing period by -0.17±0.66 day on average (Figure 7c).

[16] Finally we show a comparison between the auroral power and the variation of the interplanetary magnetic field from the Juno observation in Figure 8. The auroral power over wavelengths of 80–170 nm without absorption, estimated from the observation at 138.5–144.8 nm [Tao et al., 2016b], is shown on the right y-axis. There are significant solar wind variations on DOY 22–27, DOY 39–43, and DOY 50–59 in 2016. The lower envelope of the auroral power, i.e., the background of the periodic peaks, is correlated with the IMF variations. For example, the auroral power increases from 1.5 TW on DOY 22–23 to 3.5 TW on DOY 24–25 and then decreases to ~1 TW on DOY 30. The power variation trend is similar to that of the IMF. Periodic variations are seen in addition to these variations, e.g., DOY 22, 23, and 25 in the first enhancement. These periodic variations are continuously observed in periods of both quiet and enhanced IMF. From this observation, the auroral power amplitude associated with the solar wind is estimated to be 1–3 TW. This is comparable with the typical amplitude of the periodic variation of ~0.8 TW and that of the auroral burst of ~1 TW up to 6 TW, which are estimated from the whole dataset.

4. Discussion

4.1. Comparison with Other Studies for a Global View

[17] Quasi-periodic variations have been reported for various parameters along with their characteristics. We focus on the periodicity, asymmetric increasing and decreasing time durations, and

the time scale of auroral power variation. Here we compare our results with those of previous studies and construct a global view based on the magnetospheric reconfiguration model proposed by Woch et al. [1998] (Figure 9).

[18] The separation time of the periodic variation seen in the aurora is scattered over 0.8–8 days with a peak at 2 days. This is comparable with previous reports, i.e., 5–10 days seen in the aurora by IUE observation [Prangé et al., 2001], 1.5–7 days in plasma spectra [Kronberg et al., 2009] and in the signatures of magnetic field stretching and depolarization [Kronberg et al., 2008], and 1–4 days in magnetic-reconnection-like features [Vogt et al., 2010] and in wave power spectra [Vogt et al., 2019], and ~3 days in both magnetic field and plasma taken by Juno [Vogt et al., 2020].

[19] Our observation shows increases for a duration of 0.96±0.39 days and decreases for a duration of 0.78±0.52 days. Asymmetric durations of increases and decreases were found by in-situ plasma observations [e.g., Woch et al., 1998]. The decrease in the energetic ion flux and the increase in the spectral slope take ~2 days, while the flux increases and the slope decreases within ~1 day with disturbed features.

[20] To compare the intrinsic durations in detail, we also statistically investigated the duration of the periodic variation in the energetic ions observed by Galileo using the dataset of Kronberg et al. [2009]. Referring to the time variation of the spectral index γ of energetic ion distributions observed by Energetic Particle Detector (EPD) on board Galileo, intervals of increasing and decreasing spectral index are detected for the 71 events from 1996 to 2002. As a result, we found that the duration of increasing spectral index is 1.84±0.97 days and the duration of decreasing spectral index is 1.24±0.87 days (Figure 10). The difference between durations of spectral hardening and softening is significant according to the Mann–Whitney U-test ($U=3695$, $z=4.79$, $p=1.65\times10^{-6}$, $n=141$). The difference, i.e., the duration of decreasing subtracted by the duration of increasing, is -0.60±0.92 days. Therefore, the significant asymmetry in intervals of increasing and decreasing is confirmed in both the auroral power

(Section 3) and energetic ion spectral index γ that is related to the thinning of the plasma sheet [Kronberg et al., 2007], while the difference between the durations seen in aurora, -0.17±0.66 day, is still much smaller than the difference related to variation of energetic ion spectra.

[21] Magnetic field dipolarization and plasma sheet thinning have been observed with the periodic variation of energetic particles [e.g., Kronberg et al., 2007, Vogt et al., 2020]. They also found that the magnetic field ratio of the southward component to the radial component reaches the threshold for the ion tearing instability at the end of the stretching phase. Energetic ion bursts were sometimes but not always observed during this disturbed time. Yao et al. [2019] found the magnetic reconnection-like features, probably linked to small-scale drizzle reconnection, occur during both loading and unloading variation seen in magnetic field and plasma observed by Juno. According to their Figure 2, the occurrence of the reconnection-like feature seems to be concentrated around the end of the stretching phase and beginning of the diporalization phase. Prangé et al. [2001] found magnetic field disturbance in the magnetospheric tail around the peak of the auroral power. Interestingly, our Hisaki observation sometimes detected auroral bursts, and we found in this study that they occur at the peak of the periodic variation. These aurora bursts are associated with auroral blobs and low-latitude expansion of the main auroral oval on the basis of auroral imaging by HST [Kimura et al., 2015; Badman et al., 2016], an example of which is shown in Figure 9. Bonfond et al. [2012] reported a months-long expansion of the main emissions at the same time as the occurrence rate of intense equatorward emissions strongly increased in 2007. Yao et al. (accepted) reported that signatures of larger scale reconnection have been related to large auroral brightening seen in the dawnside which is called dawn storms. These auroral structures are considered to represent the Jupiter's reconfiguration events. The stretching of the magnetosphere and energy exploration process in the tail region (e.g., reconnections) initiate auroral bursts. Inversely, auroral bursts provide an opportunity for monitoring reconfiguration events.

[22] Note that the magnetospheric reconnection-like feature and in-situ ion bursts are observed several times within one periodic variation [e.g., Kronberg et al., 2007, Yao et al., 2019]. This multiple feature

would be related with the several auroral spots which appearing and disappearing with a period of 2–3 days [Radioti et al., 2010]. On the other hand, the auroral burst observed by Hisaki's polar-integrated view would be sum and/or their developed feature of them.

[23] In the following sections, we will quantitatively discuss the auroral variation and Io's volcanic activity and solar wind effects within this global view.

4.2. Quantitative Analysis of Auroral Variation

[24] The results of superposed-epoch analysis shown in Figure 6 suggests that the periodic variation of auroral emission is associated with the increase in auroral source current. Tao et al. [2016b] quantitatively evaluated the variation of auroral emission due to (i) a magnetospheric compression and (ii) a change in the relative contribution of different components in the auroral structures as possible explanations of the auroral variation during solar wind compressions and/or plasma injections. On the other hand, the periodic variation in the global feature (Section 4.1) is considered to correspond to the plasma sheet thinning phase rather than the radial compression for (i). The change in the auroral components, (ii), is also unlikely to be the cause of this variation. Here we consider a quantitative estimation for this case of plasma sheet thinning.

[25] The source current density $j_{//0}$ $(2.5/k_B T_0$ [keV]$) \propto N_0 {T_0}^{-1/2}$ (see Tao et al. [2016b] for details) is the current density conveyed without acceleration by magnetospheric electrons with density N_0 and temperature T_0. Here we also assume adiabaticity, i.e., $PV^{\gamma} = \text{constant}$ with γ = 5/3, where $P = N_0 k_B T_0$ is the plasma pressure, V is the flux tube volume (i.e., the volume per unit magnetic flux), and k_B is the Boltzmann constant. From the mass conservation, VN_0 =constant, we obtain $j_{//0} \propto N_0\left({N_0}^{\gamma-1}\right)^{-1/2} = {N_0}^{2/3}$. Referring to the observed ~1.6-fold increase in the source current (Figure 6f), the plasma density is estimated to increase by a factor of $1.6^{3/2}$=2.0 and the pressure variation by a factor of $1.6^{3/2+1}$= 3.2. From the mass conservation, VN_0 = constant, the volume will be decreased by 50%. This can be achieved by, for example, a change in the dimensions of the initial region from Δ15

R_J in the radial direction with width Δ4 R_J in the north-south direction to those of Δ30 R_J and Δ1 R_J width, respectively, in the thinning phase at the similar radial distance.

[26] Kronberg et al. [2007] evaluated the magnetic field variation during the periodic variation from the results of in-situ observation. They obtained a radial component of B_r=3.5 nT and a meridional component of B_θ=1.1 nT in the mass-unloaded phase and values of B_r=4.5 nT and B_θ=0.1 nT in the reconnection phase. This suggests an increase in magnetic pressure by a factor of 1.5. Some events showed a variation from B_r=3 nT to 6 nT (Figure 1 of Kronberg et al. [2007]) resulting in the magnetic pressure increasing by a factor of ~3.5. The plasma thermal pressure is almost balanced with the magnetic pressure in the Jupiter magnetotail, as also shown by Kronberg et al. [2007]. Note that the magnetic field variation was observed at magnetotail ~120 R_J, while the auroral source current mainly reflects the middle magnetosphere ~30–50 R_J. Referring to the periodic variation in the plasma pressure investigated by Kronberg et al. [2008], the pressure varies by a factor of 2.5–5.5 at 30–60 R_J. The 3.2-fold pressure enhancement estimated from this study is comparable with the observed variation. Therefore the auroral periodic variation is quantitatively linked with the source current variation due to magnetospheric plasma thinning and dipolarization.

4.3. Modulations by Io Volcanic Activity: Periodicity

[27] Our analysis does not show a significant difference in the periodicity of the volcanic activity of Io. On the other hand, decreasing time constant of the Jovian magnetosphere needed for mass loading with increasing plasma mass flux has been proposed by Kronberg et al. [2007] on the basis of a quantitative relationship. Here we estimate the expected variation of the periodicity from the relationship and its detectability using our dataset.

[28] Assuming a pressure balance with appropriate simplifications for the Jupiter magnetotail environment, Kronberg et al. [2007] defined a parameter representing the plasma sheet topology. They

obtained the periodic time constant τ from the time variation of the parameter. One of their proposed relationships relating the τ with the plasma mass flux is as follows:

$$\tau \simeq \frac{\rho_{rec}-\rho_0}{\dot{\rho}} \propto \frac{\delta n}{\dot{\rho}}, \qquad (1)$$

where the ρ_{rec} and ρ_0 are the plasma mass density just before the reconnection and that at the start of the mass-loading phase, respectively; $\dot{\rho} = \dot{m}/V_{PS}$, where $\dot{m}$ is the mass-loading rate and V_{ps} is the mass-loaded plasma sheet volume; and $\delta n = \frac{(\rho_{rec}-\rho_0)}{16 m_p}$ is the number density, where m_{p} is the proton mass. For δn = 0.05, referring to the plasma observation by Frank et al. [2002], the time constant is estimated to be 6.5–1 days for the probable mass-loading rate of 100–600 kg/s and ~2.5 days for the most likely value of the mass-loading rate of 250 kg/s.

[29] Io's volcanic activity in 2015 was distinct from the past events seen in the sodium nebula reaching 60 kR at 50 R_J compared with 20–25 kR before this event [Yoneda et al., 2015]. From IPT spectral analysis combined with a chemical model, it was found that the net production of S and O increases from 700±130 kg/s to 3000±300 kg/s (~4.3 times) and the electron density increases from 2350±340 cm^{-3} to 2860±260 cm^{-3} (~1.2 times) at ~6 R_J around the peak of the volcanic event compared with a quiet time [Yoshioka et al., 2018]. Their analysis also suggested that plasma outflow velocity increases by ~3.4 times during the volcanically active time. Hikida et al. [2020] applied the plasma diagnosis method to the Hisaki data with the 140 arcsec slit and obtained a similar electron variation from 1790±80 /cc to 2400±100 /cc (~1.3 times) during the volcanic event. An analytic method considering conservations of the magnetic flux and energy in the interchange motion at the IPT associated with the IPT emission observed by Hisaki suggests an increase in the plasma mass-loading rate from 300 to 500 kg/s (1.66 times) during this volcanic event [Kimura et al., 2018]. Auroral spectral analysis combined with the auroral particle acceleration theory suggests that the source plasma density around the middle magnetosphere also increases from 0.0019 to 0.0027 /cm^3 (1.4 times) [Tao et al., 2018].

Increases in the plasma density and mass-loading rate by factors of 1.2–1.7 are estimated from these various methods.

[30] For the variation of the mass-loading rate from 300 to 500 kg/s [Kimura et al., 2018], relationship (1) with δn = 0.05 corresponds to a decrease in the time constant from 2 to 1.2 days. The difference between the maximum and minimum values is 0.8 day. For the increase in the plasma density and mass-loading rate by a factor of 1.2–1.7, the decrease in the time constant is ~83–60%. If the time constant at the volcanically quiet condition is 3 days, that at the active condition is expected to be in the range of 2.5–1.8 days. The difference between quiet and active conditions is 0.50–1.2 days.

[31] Here, we analyzed the power, i.e., probability to detect the significant difference correctly, of our test using the wmwpow package (ver. 0.1.2, R). This package evaluates the exact power of the Mann–Whitney U-test using a Monte Carlo approach [Mollan et al., 2019]. The obtained detection power was 0.83 (0.81) with a potential difference of 1.25 (1.2) days for the event number of our dataset, which is comparable to a generally acceptable value of 0.8. From our analysis, the difference between the volcanic quiet (dt=3.0 day) and active conditions (dt=2.6 day) was 0.4 days (Section 3), which is less than 1.25 day. Therefore, a difference of greater than 1.25 days is unlikely to exist between the active and quiet conditions. This also indicates that our dataset is not adequate for detecting a difference of less than 1.25 days. The expected difference of 0.50–1.2 days for this volcanic event is beyond this detection ability.

[32] The power for a smaller difference improves with increasing number of samples. If the observed separation times on DOY 10–200 in 2016 are added as the quiet period, the number of samples for the quiet time increases to 43. With the 19 samples during the volcanically active time, the dataset has a large power (0.889) for detecting a difference of 1.2 days but insufficient power to detect a difference of 0.5 days (power of 0.261) according to the wmwpow analysis. In addition, the obtained mean values of the two groups become closer, 2.65 and 2.62, for the quiet and active conditions, respectively.

[33] Therefore, a significant difference in periodicity between volcanically quiet and active conditions is not derived from our dataset. From the detection analysis, we cannot conclude whether no difference exists or whether a difference of less than 1.25 days exists. Further observations are expected to answer this remaining question.

4.4. Modulations by Io Volcanic Activity: Auroral Burst

[34] The occurrence of aurora bursts increased significantly during enhanced volcanic activity as also previously reported [Yoshikawa et al., 2017; Tsuchiya et al., 2018; Kimura et al., 2018, Tao et al., 2018]. In addition, a new finding in this study is the correlation between the auroral burst power and the power of the periodic amplitude. This correlation indicates that the explosion of the magnetospheric power is related to the activity of the background periodic variation. These bursts are considered to be the main contributor to the plasma mass release via magnetospheric reconnection.

4.5 Modulations by Solar Wind

[35] As seen in the comparison of the periodic variation obtained with Juno's IMF observation, the periodic variation continues under solar wind compression events. This supports the independent periodic variation of the energetic particle flux and spectral slope proposed by Kronberg et al. [2008] and Vogt et al. [2019]. From the statistical analysis using the plasma and magnetic field datasets measured by Galileo, Vogt et al. [2019] found that increases in the solar wind dynamic pressure are statistically associated with magnetospheric compression events while tail reconnection and plasmoid release are most likely internally driven by the Vasyliunas cycle. Our results of auroral observation also reflect these two characteristic dynamics. As shown in Figure 8, the increasing trend of the auroral base over several days closely reflects the variation of the IMF strength. This power modulation is probably due to magnetospheric compression. Similar auroral variation was reported in Hisaki observation by e.g., Kita et al. [2016] and Tao et al. [2016b], referring to the solar wind variation estimated by model [Tao et al., 2005]. Using HST image taken in May-June 2016, Nichols et al. [2017]

reported that main emissions and duskside poleward region are brightened during the solar wind compressions observed by Juno. On the other hand, the quasi-periodic variation and auroral bursts at these peaks sometimes correspond to the auroral reconnection and plasmoid release as discussed in Section 4.1. Our dataset of polar total auroral power is unique in its reflection of both types of dynamics. The relative contribution of both dynamics to the total power is derived from this study, i.e., the intrinsic periodic variation provides ~0.8 TW amplitude with an auroral burst of 1–6 TW and is comparable to the 1–3 TW contribution from solar wind variation. This auroral power modulated by solar wind is comparable with those observed in May–June 2016 [e.g., Gladstone et al., 2017, Nichols et al., 2017, Kita et al., 2019].

5. Summary

[36] We have investigated the quasi-periodic variation of polar-*integrated* auroral power with a period of a few to several days using observation by the Hisaki space telescope from the end of 2013 to the middle of 2016. From our analysis, we obtained the following results.

[37] (1) The detected periodicity of the auroral power is 0.8–8 days with a peak at 2 days. The increasing duration of the periodic auroral variation is slightly but significantly longer than the decreasing duration on average, as seen with the in-situ plasma observation by Galileo.

[38] (2) Significant difference in the periodicity depending on the volcanic activity for the active period in early 2015 was not detected in our dataset, partly because of the insufficient amount of data to detect the expected difference from the theoretical estimation applied for this volcanic event. On the other hand, our dataset suggests that a difference greater than 1.25 days is unlikely to exist between the volcanically active and quiet conditions, which is consistent with the expected difference estimated from a proposed relationship applied to the plasma variation of this volcanic event.

[39] (3) The periodic variation is mainly caused by the total auroral electron flux variation rather than the averaged auroral energy variation. This variation is associated with magnetospheric thinning by quantitative comparison with the in-situ observation.

[40] (4) Auroral bursts within short durations <10 h and a large amplitude were sometimes found at the peaks of the periodic variation. A positive correlation was found between the auroral burst power and the periodic amplitude. The occurrence of the auroral bursts was 41% of periodic peaks during the volcanically quiet time, which increased to 65% during the volcanically active time.

[41] (5) The periodic variation associated with the auroral bursts was continuously seen when solar wind structures hit the magnetosphere. The variation associated with solar wind is 1–3 TW, the periodic variation is ~0.8 TW, and the auroral burst varies from ~1 TW to 6 TW.

[42] The time variation of the aurora suggests a link to other previous observations and theoretical models associated with the magnetospheric reconfiguration. Remaining and newly proposed questions for future works are as follows. Which spatial component(s) of the aurora is responsible for the periodic variation? Does the periodicity depend on the variation in the plasma density and/or the mass-loading rate? What determines the occurrence and absence of the bursts? For the third question, one possibility is the amount of accumulated plasma [e.g., Kimura et al., 2018], and another is the geometry of the plasma sheet and its condition towards reconnection-associated instabilities. Why is the asymmetry of the increasing and decreasing durations in auroral power less than that of the periodic variation of in-situ energetic ions? The reflection of global regions in auroral observations compared with the locality for in-situ observations and/or the time variation between Hisaki and Galileo observations might be related to this difference.

[43] These Hisaki observations provide a total power variation without resolving auroral spatial distribution as achieved by Juno and HST. In spite of limited spatial resolution, this study revealed that

this Hisaki dataset can monitor the global internal dynamics of periodic variations and associated auroral bursts.

Acknowledgements

[44] We acknowledge the working teams of Hisaki/EXCEED and Juno. The data from the Hisaki spacecraft can be found in the Data Archives and Transmission System (DARTS) of JAXA at https://www.darts.isas.jaxa.jp/stp/hisaki/. The Juno magnetometer (MAG) data were taken from the NASA PDS website (https://pds.nasa.gov/). Auroral images was taken from observations made with the NASA/ESA Hubble Space Telescope (observation ID: GO13035), obtained at the Space Telescope Science Institute, which is operated by AURA, Inc. for NASA. The Galileo EPD data can be also found in NASA PDS website (https://pds.nasa.gov/). We acknowledge Dr. Andreas Lagg for the use of his software to analyze the Galileo EPD data. This work was supported by MEXT/JSPS KAKENHI Grant 19H01948. EK is supported by German Research Foundation (DFG) under number KR 4375/2-1 within SPP “Dynamic Earth”. MFV was supported by NASA Grant 80NSSC17K0777 as part of the Solar System Workings program and by the National Science Foundation under Award 1524651. We acknowledge the contribution of the International Space Sciences Institute (ISSI) in Bern, Switzerland, for hosting and funding the ISSI international teams on “The influence of Io on Jupiter’s magnetosphere” (ID388) and “How does the solar wind influence the giant planet magnetospheres?” (ID357) and the constructive discussions had by these team members. We also thank NASA-Hisaki PSP members for useful discussions.

References

Badman, S. V., et al. (2016), Weakening of Jupiter's main auroral emission during January 2014, Geophys. Res. Lett., 43, 988–997, doi:10.1002/2015GL067366.

Bonfond, B., D. Grodent, J.-C. Gérard, T. Stallard, J. T. Clarke, M. Yoneda, A. Radioti, and J. Gustin (2012), Auroral evidence of Io’s control over the magnetosphere of Jupiter, Geophys. Res. Lett., 39, L01105, doi:10.1029/2011GL050253.

Connerney, J. E. P., et al. (2017), The Juno magnetic field investigation, Space Sci. Rev., 213:39–138, DOI 10.1007/s11214-017-0334-z.

Frank, L. A., W. R. Paterson, and K. K. Khurana (2002), Observations of thermal plasmas in Jupiter's magnetotail, J. Geophys. Res., 107(A1), 1003, doi:10.1029/2001JA000077.

Gladstone, G. R., et al. (2017), Juno-UVS approach observations of Jupiter's auroras, Geophys. Res. Lett., 44, 7668–7675, doi:10.1002/2017GL073377.

Gray, R. L., S. V. Badman, B. Bonfond, T. Kimura, H. Misawa, J. D. Nichols, M. F. Vogt, and L. C. Ray (2016), Auroral evidence of radial transport at Jupiter during January 2014, J. Geophys. Res. Space Physics, 121, 9972–9984, doi:10.1002/2016JA023007.

Hikida, R., Yoshioka, K., Tsuchiya, F., Kagitani, M., Kimura, T., Bagenal, F., et al. (2020), Spatially asymmetric increase in hot electron fraction in the Io plasma torus during volcanically active period revealed by observations by Hisaki/EXCEED from November 2014 to May 2015, J. Geophys. Res.: Space Phys., 125, e2019JA027100. https://doi.org/10.1029/2019JA027100

Kimura, T., et al. (2015), Transient internally driven aurora at Jupiter discovered by Hisaki and the Hubble Space Telescope, *Geophys. Res. Lett.*, *42*, doi:10.1002/2015GL063272.

Kimura, T., et al. (2017), Transient brightening of Jupiter's aurora observed by the Hisaki satellite and Hubble Space Telescope during approach phase of the Juno spacecraft, Geophys. Res. Lett., 44, doi:10.1002/2017GL072912.

Kimura, T., Hiraki, Y., Tao, C., Tsuchiya, F., Delamere, P. A., Yoshioka, K., et al. (2018). Response of Jupiter's aurora to plasma mass loading rate monitored by the Hisaki satellite during volcanic eruptions at Io. Journal of Geophysical Research: Space Physics, 123. https://doi.org/10.1002/2017JA025029.

Kimura, T., A. Yamazaki, K. Yoshioka, G. Murakami, F. Tsuchiya, H. Kita, C. Tao, I. Yoshikawa, A. Kumamoto, and C. Yamauchi (2019), Development of ground pipeline system for high-level scientific data products of the Hisaki satellite mission and its application to planetary space weather, J. Space Weather Space Clim., 9, A8 (pp1-14).

Kita, H., et al. (2016), Characteristics of solar wind control on Jovian UV auroral activity deciphered by long-term Hisaki EXCEED observations: Evidence of preconditioning of the magnetosphere?, Geophys. Res. Lett., 43, doi:10.1002/2016GL069481.

Kita, H., Kimura, T., Tao, C., Tsuchiya, F., Murakami, G., Yamazaki, A., et al. (2019). Jovian UV aurora's response to the solar wind: Hisaki EXCEED and Juno observations. J. Geophys. Res.: Space Phys., 124, https://doi.org/10.1029/2019JA026997.

Kronberg, E. A., K.-H. Glassmeier, J. Woch, N. Krupp, A. Lagg, and M. K. Dougherty (2007), A possible intrinsic mechanism for the quasi-periodic dynamics of the Jovian magnetosphere, J. Geophys. Res., 112, A05203, doi:10.1029/2006JA011994.

Kronberg, E. A., J. Woch, N. Krupp, A. Lagg, P. W. Daly, and A. Korth (2008), Comparison of periodic substorms at Jupiter and Earth, J. Geophys. Res., 113, A04212, doi:10.1029/2007JA012880.

Kronberg, E. A., J. Woch, N. Krupp, and A. Lagg (2009), A summary of observational records on periodicities above the rotational period in the Jovian magnetosphere, Ann. Geophys. 27, 2565-2573.

Louarn, P., C. P. Paranicas, and W. S. Kurth (2014), Global magnetodisk disturbances and energetic particle injections at Jupiter, J. Geophys. Res. Space Physics, 119, doi:10.1002/2014JA019846.

Mollan, K. R., I. M. Trumble, S. A. Reifeis, O. Ferrer, C. P. Bay, P. L. Baldoni, and M. G. Hudgens (2019), Exact power of the rank-sum test for a continuous variable, arXiv:1901.04597v1.

Nichols, J. D., et al. (2017), Response of Jupiter’s auroras to conditions in the interplanetary medium as measured by the Hubble Space Telescope and Juno, Geophys. Res. Lett., 44, 7643–7652, doi:10.1002/2017GL073029.

Prangé, R., G. Chagnon, M. G. Kivelson, T. A. Livengood, and W. Kurth (2001), Temporal monitoring of Jupiter’s auroral activity with IUE during Galileo mission. Implications for magnetospheric processes, Planet. Space Sci., 49, 405-415.

Radioti, A., D. Grodent, J.-C. Gérard, and B. Bonfond (2010), Auroral signatures of flow bursts released during magnetotail reconnection at Jupiter, J. Geophys. Res., 115, A07214, doi:10.1029/2009JA014844.

Tao, C., R. Kataoka, H. Fukunishi, Y. Takahashi, and T. Yokoyama (2005), Magnetic field variations in the Jovian magnetotail induced by solar wind dynamic pressure enhancements, J. Geophys. Res., 110, A11208, doi:10.1029/2004JA010959.

Tao, C., et al. (2016a), Variation of Jupiter's aurora observed by Hisaki/EXCEED: 1. Observed characteristics of the auroral electron energies compared with observations performed using HST/STIS, *J. Geophys. Res. Space Physics, 121*, 4041–4054, doi:10.1002/2015JA021271.

Tao, C., T. Kimura, S. V. Badman, N. André, F. Tsuchiya, G. Murakami, K. Yoshioka, I. Yoshikawa, A. Yamazaki, and M. Fujimoto (2016b), Variation of Jupiter's aurora observed by Hisaki/EXCEED: 2. Estimations of auroral parameters and magnetospheric dynamics, *J. Geophys. Res. Space Physics, 121*, 4055–4071, doi:10.1002/2015JA021272.

Tao, C., Kimura, T., Tsuchiya, F., Muirakami, G., Yoshioka, K., Yamazaki, A., … Fujimoto, M. (2018). Variation of Jupiter's aurora observed by Hisaki/EXCEED: 3. Volcanic control of Jupiter's aurora. Geophysical Research Letters, 45, 71–79. https://doi.org/10.1002/2017GL075814.

Tsuchiya, F., Yoshioka, K., Kimura, T., Koga, R., Murakami, G., Yamazaki, A., et al. (2018). Enhancement of the Jovian magnetospheric plasma circulation caused by the change in plasma supply from the satellite Io. Journal of Geophysical Research: Space Physics, 123, 6514–6532. https://doi.org/10.1029/2018JA025316.

Tsuchiya, F., Arakawa, R., Misawa, H., Kagitani, M., Koga, R., Suzuki, F., et al. (2019), Azimuthal variation in the Io plasma torus observed by the Hisaki satellite from 2013 to 2016, J. Geophys. Res.: Space Phys., 124, 3236–3254. https://doi.org/10.1029/2018JA026038

Vasyliunas, V. M. (1983), Plasma distribution and flow, in *Physics of the Jovian Magnetosphere*, edited by A. J. Dessler, pp. 395– 453, Cambridge Univ. Press, New York.

Vogt, M. F., M. G. Kivelson, K. K. Khurana, S. P. Joy, and R. J. Walker (2010), Reconnection and flows in the Jovian magnetotail as inferred from magnetometer observations, J. Geophys. Res., 115, A06219, doi:10.1029/2009JA015098.

Vogt, M. F., Gyalay, S., Kronberg, E. A., Bunce, E. J., Kurth, W. S., Zieger, B., & Tao, C. (2019). Solar wind interaction with Jupiter's magnetosphere: A statistical study of Galileo in situ data and modeled upstream solar wind conditions. Journal of Geophysical Research: Space Physics, 124, 10,170-10,199, https://doi.org/10.1029/2019JA026950.

Vogt, M. F., Connerney, J. E. P., DiBraccio, G. A., Wilson, R. J., Thomsen, M. F., Ebert, R. W., et al. (2020). Magnetotail reconnection at Jupiter: A survey of Juno magnetic field observations. J. Geophys. Res.: Space Phys., 125, e2019JA027486. https://doi.org/10.1029/2019JA027486.

Wilson, R. J., Bagenal, F., Valek, P. W., McComas, D. J., Allegrini, F., Ebert, R. W., et al. (2018). Solar wind properties during Juno's approach to Jupiter: Data analysis and resulting plasma properties utilizing a 1-D forward model. J. of Geophys. Res.: Space Phys., 123, 2772–2786. https://doi.org/10.1002/2017JA024860

Woch, J., N. Krupp, A. Lagg, B. Wilken, S. Livi, and D. J. Williams (1998), Quasi-periodic modulations of the Jovian magnetotail, Geophys. Res. Lett., 25, 8, 1253–1256, https://doi.org/10.1029/98GL00861.

Yamazaki, A. et al. (2014), Field-of-view guiding camera on the HISAKI (SPRINT-A) satellite, *Space Sci. Rev., 184,* 1–4, 259–274, DOI: 10.1007/s11214-014-0106-y.

Yao, Z. H., Grodent, D., Kurth, W. S., Clark, G., Mauk, B. H., Kimura, T., et al. (2019). On the relation between Jovian aurorae and the loading/unloading of the magnetic flux: Simultaneous measurements from Juno, Hubble Space Telescope, and Hisaki. Geophys. Res. Lett., 46, https://doi.org/10.1029/2019GL084201.

Yao, Z. H, B. Bonfond, G. Clark, D. Grodent, W. R. Dunn, M. F. Vogt, R. L. Guo, B. H. Mauk, J. E. P. Connerney, S. M. Levin, and S. J. Bolton, Reconnection and Dipolarization Driven Auroral Dawn Storms and Injections, JGR, accepted, available at https://www.essoar.org/pdfjs/10.1002/essoar.10503657.1

Yoneda, M., M. Kagitani, F. Tsuchiya, T. Sakanoi, and S. Okano (2015), Brightening event seen in observations of Jupiter's extended sodium nebula, *Icaurs*, *261*, 31–33

Yoshikawa, I. et al. (2014), Extreme ultraviolet radiation measurement for planetary atmospheres/magnetospheres from the earth-orbiting spacecraft (Extreme Ultraviolet Spectroscope for Exospheric Dynamics: EXCEED), *Space Sci. Rev., 184,* 1–4, 237–258, DOI:10.1007/s11214-014-0077-z.

Yoshikawa, I. et al. (2017), Volcanic activity on Io and its influence on the dynamics of the Jovian magnetosphere observed by EXCEED/Hisaki in 2015, Earth, Planets and Space--Frontier Letter, 69, 110, doi:10.1186/s40623-017-0700-9.

Yoshioka, K. et al. (2013), The extreme ultraviolet spectroscope for planetary science, EXCEED, *Planet. Space Sci., 85,* 250–260.

Yoshioka, K., Tsuchiya, F., Kagitani, M., Kimura, T., Murakami, G., Fukuyama, D., et al. (2018). The influence of Io's 2015 volcanic activity on Jupiter's magnetospheric dynamics. Geophysical Research Letters, 45, 10,193–10,199. https://doi.org/10.1029/2018GL079264.

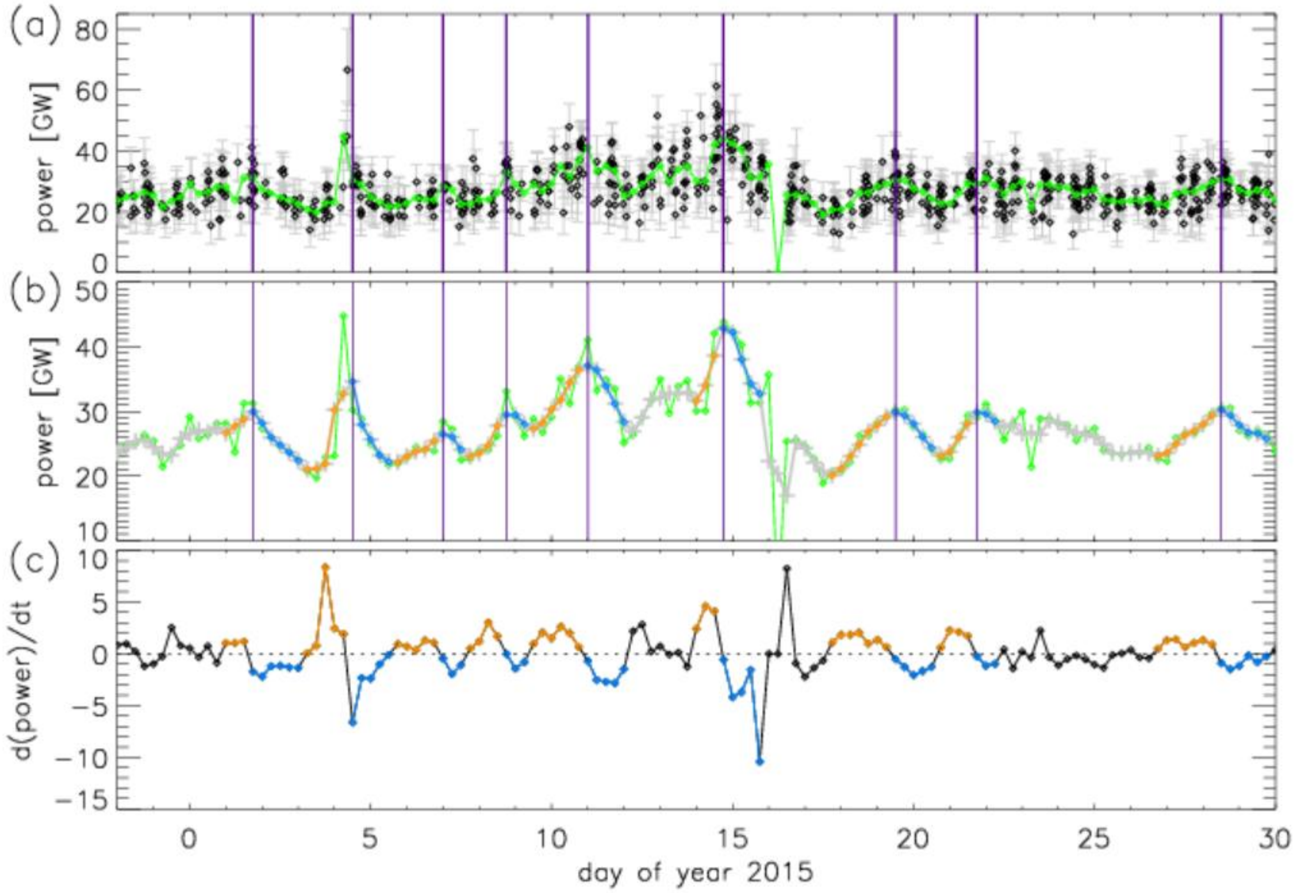

Figure 1. Time variations of (a) the auroral power emitted at wavelengths of 138.5–144.8 nm (black diamonds) and its median within the 0.5-day window shifted by 0.25 day (green line), (b) the same median power (green) and its 0.75-day (3-point) running average (grey line), and (c) time deviation of the power from December 29, 2014 to January 30, 2015. The detected positive and negative intervals continuing for ≥0.5 day are shown by orange and blue colours, respectively, in Figures 1b and 1c. Grey vertical lines in Figures 1a show errors estimated from the photon statistics. Purple vertical lines in Figures 1a and 1b represent the peak time of the quasi-periodic event detected automatically.

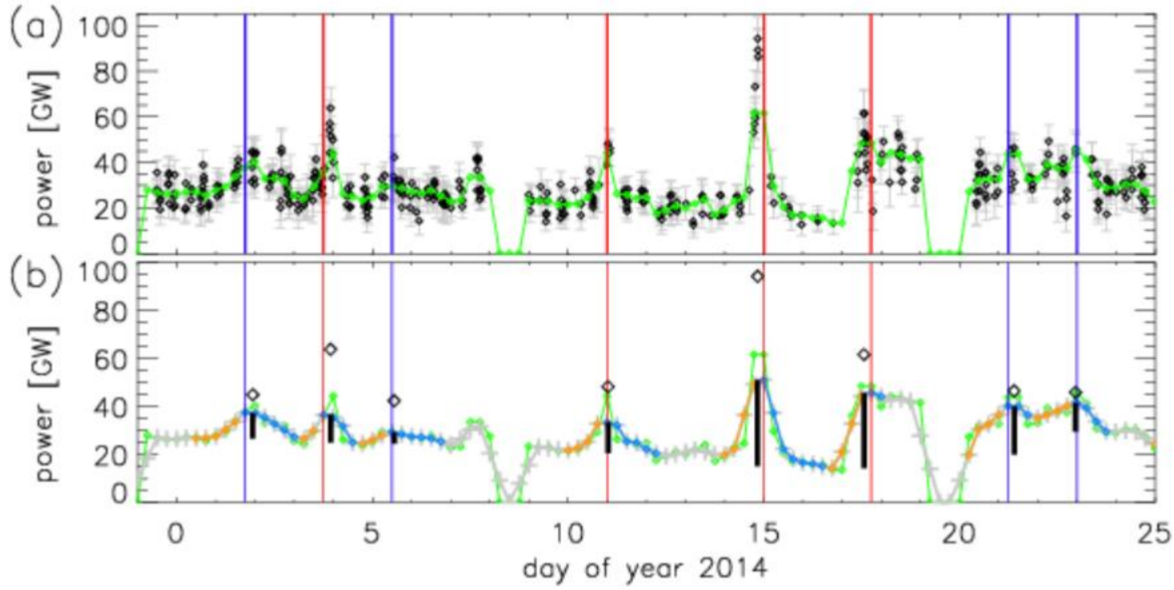

Figure 2. As Figures 1a and 1b but from December 30, 2013 to January 24, 2014. The black vertical lines in Figure 2b show the detected amplitudes of the periodic variation, and diamonds show the largest power during each enhancement. Red and blue lines represent the existence and absence of significant auroral enhancement, respectively.

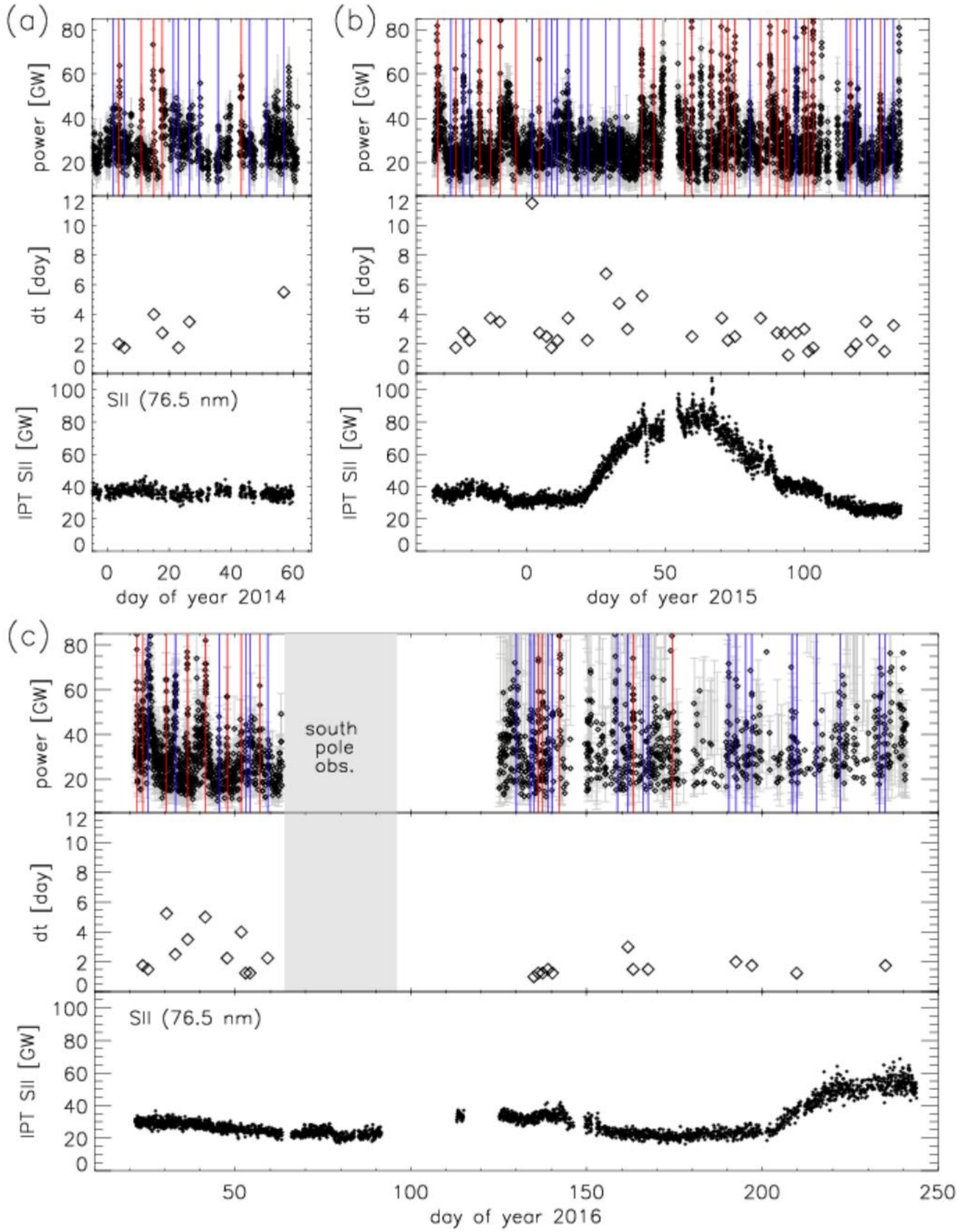

Figure 3. Time variations of the power emitted at wavelengths of 138.5–144.8 nm (upper), interval of events dt (middle), and IPT SII emission intensity (bottom, see Yoshikawa et al., 2017 for details), observed in (a) 2014, (b) 2015, and (c) 2016. Grey vertical lines in the upper plots show errors estimated from the photon statistics, and red and blue vertical lines represent the peak times of periodic events with and without significant enhancement, respectively.

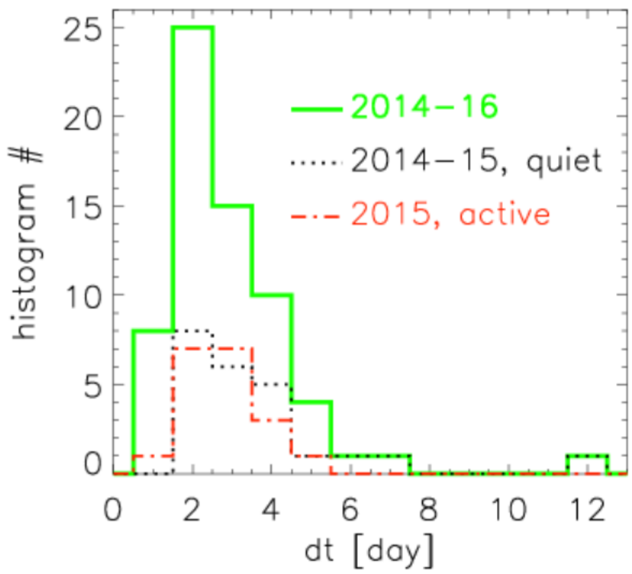

Figure 4. Histogram of separation interval *dt* of periodic events for all the 2014–2016 dataset (green line), Io’s volcanically quiet time in 2014–2015 (black dotted line), and Io’s volcanically active time in 2015 (red dot-dashed line).

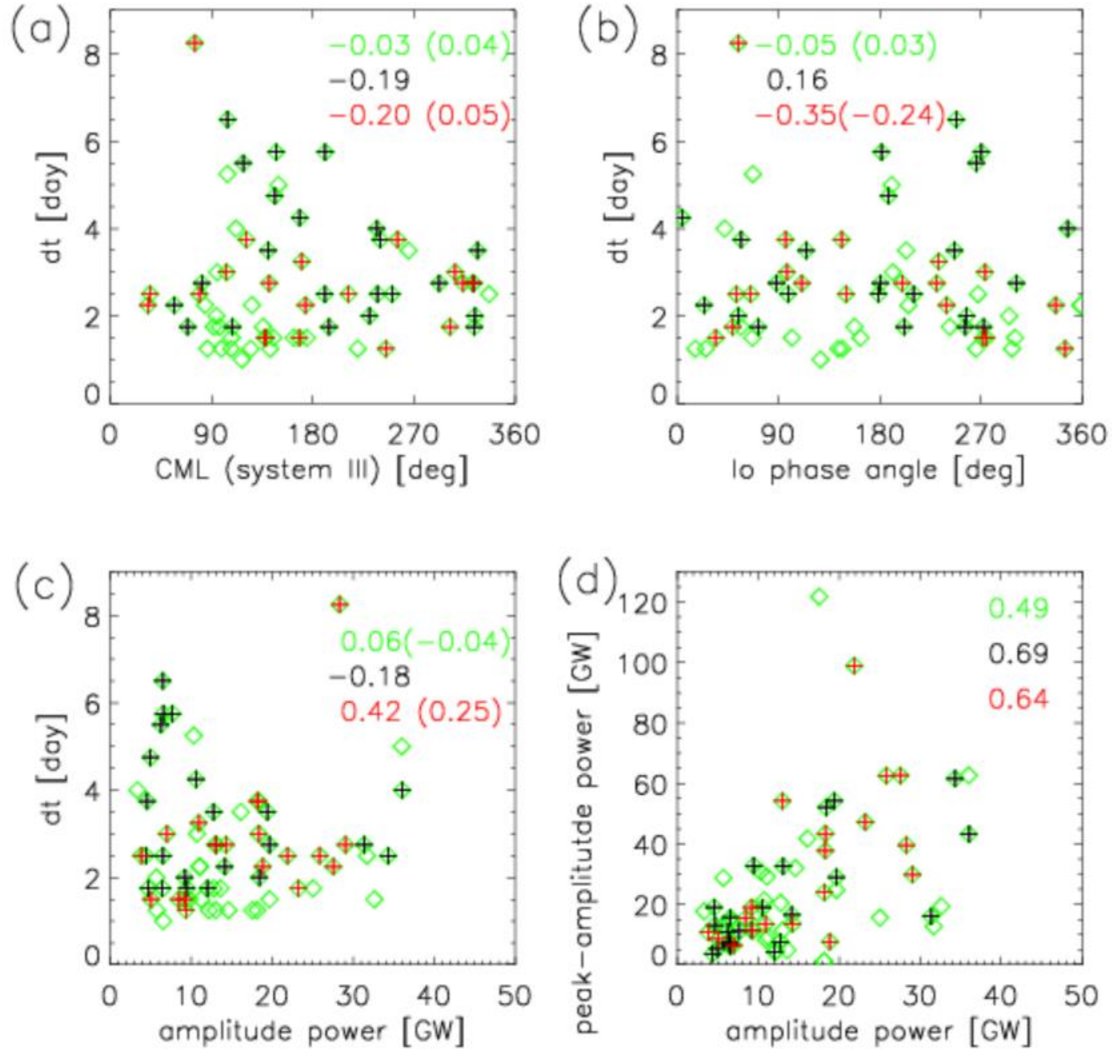

Figure 5. Separation interval *dt* as a function of (a) CML, (b) Io phase angle, and (c) amplitude power of the periodic variation, and (d) correlation between amplitude power and peak-amplitude power, for all the dataset over 2014–2016 (green diamonds), Io's volcanically quiet time (black pluses), and volcanically active time (red pluses). Numbers in the upper part of each plot are the correlation coefficient, and those in brackets are the correlation coefficients excluding the extreme case with *dt* > 8 days.

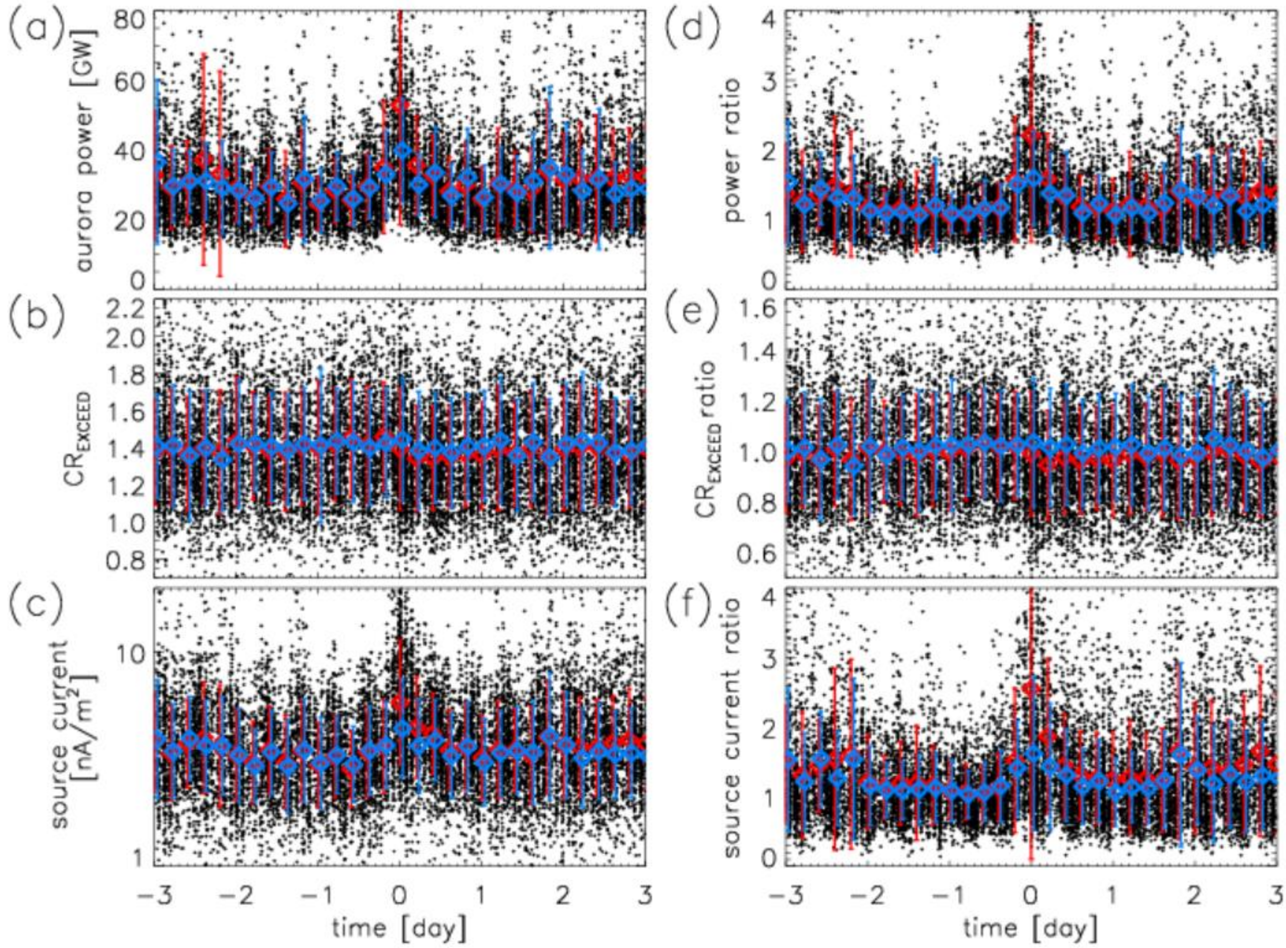

Figure 6. Results of superposed-epoch analysis for the periodic events showing (a) auroral power at 138.5–144.8 nm with rotational modulation correction, (b) CR_{EXCEED}, and (c) maximum field-aligned current that can be carried by precipitating magnetospheric electrons without field-aligned acceleration, and superposed-epoch analysis showing relative increase (see detail in text) of (d) auroral power, (e) CR_{EXCEED}, and (f) field-aligned current. The mean value within each 0.2-day bin for all events and that for events without bursts are shown by red and blue diamonds, respectively, with error bars showing the variance.

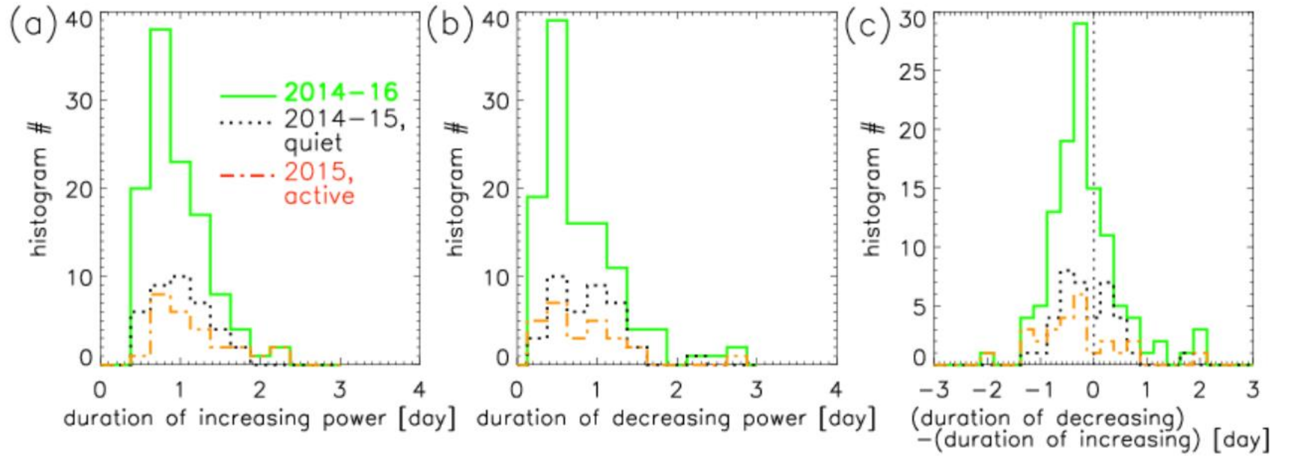

Figure 7. Histogram for the (a) durations of increasing power, (b) decreasing power, and (c) their difference in periodic events for the entire 2014–2016 dataset (solid green line), Io's volcanic quiet time in 2014–2015 (black dotted line), and Io's volcanic active time in 2015 (orange dot-dashed line).

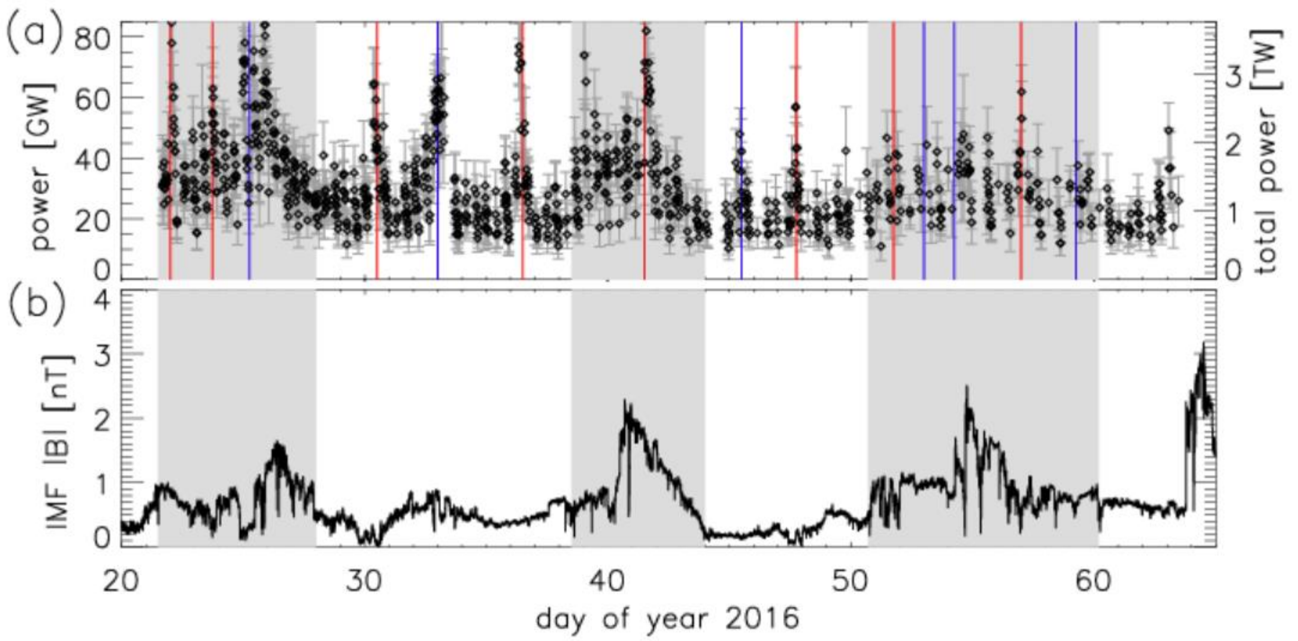

Figure 8. Time variations of (a) auroral powers emitted at wavelengths of 138.5–144.8 nm and (b) interplanetary magnetic field strength observed by Juno for DOY 20–64 in 2016. In Figure 8a, grey vertical lines show errors estimated from the photon statistics, and red and blue vertical lines represent the peak times of periodic events with and without auroral bursts, respectively. The right y-axis in Figure 8a shows the auroral power over wavelengths of 80–170 nm without absorption. Grey hatched regions are solar wind events.

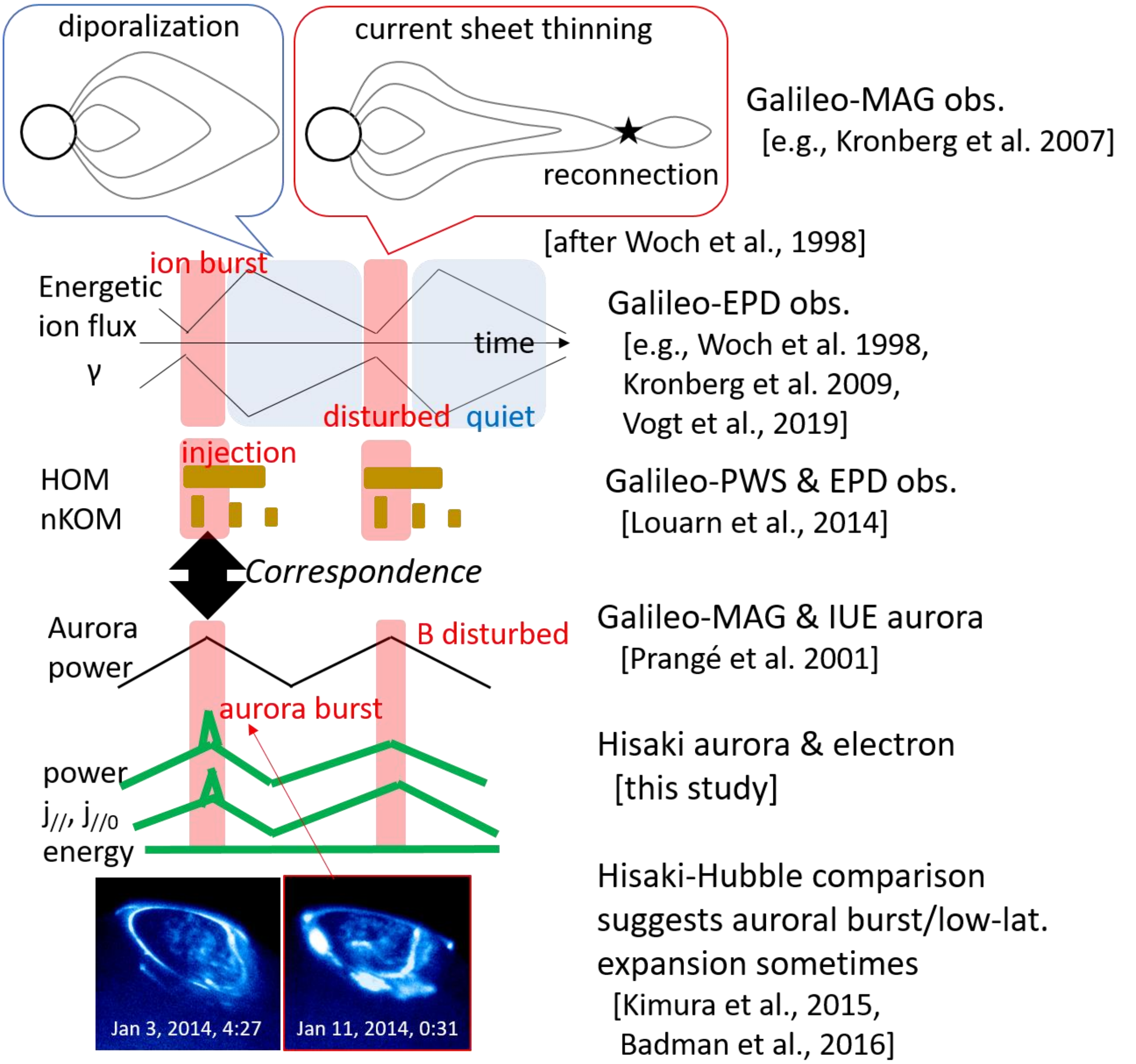

Figure 9. Schematics representing from top to bottom the magnetospheric reconfiguration model and the related observed characteristics of the energetic ion flux and spectral index γ; the auroral radio emissions; the auroral power from previous observation; the auroral power, flux, and energy from this study; and auroral images taken by HST at quiet (left) and disturbed (right) times.

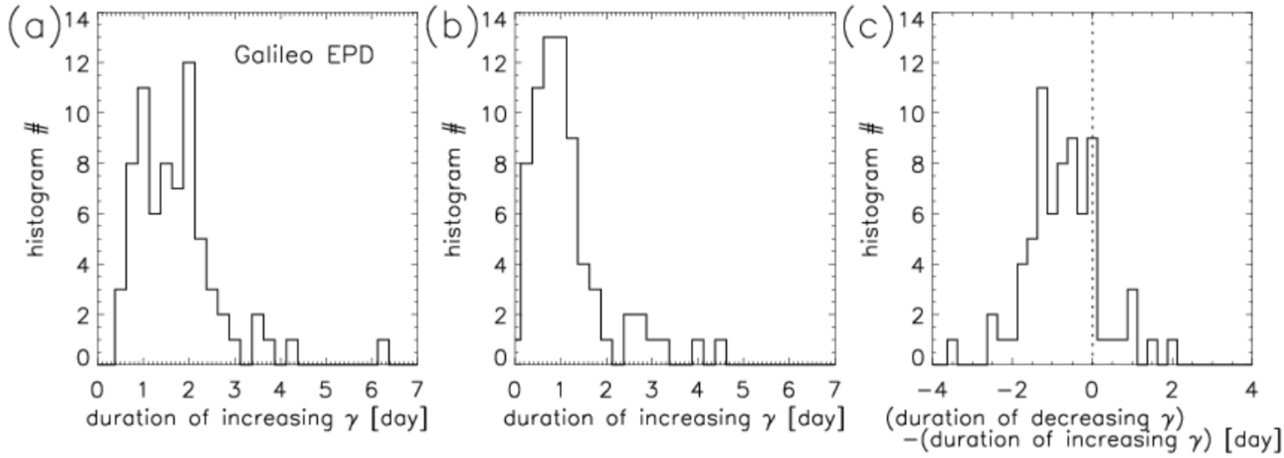

Figure 10. Histograms for the (a) durations of increasing and (b) decreasing spectral index γ of energetic ion distributions and (c) their difference observed by the Galileo EPD.